Latin American Journal of
Solids and Structures
www.lajss.org

Free Vibration Analysis of Orthtropic Thin Cylindrical Shells with Variable Thickness by Using Spline Functions

Abstract

In this study, vibration behavior of orthotropic cylindrical shells with variable thickness is investigated. Based on linear shell theory and applying energy method and using spline functions, free vibration relations are derived for shell with variable thickness and curvature. Frequency parameter and mode shapes are found after solving the frequency Eigenvalue equation. Effects of variable thickness along axial and circumferential directions of the shell on its frequency parameter are studied and compared against each other. Shell thickness is assumed to be varied in a parabolic profile along both directions. Also, frequency parameters for both circular and parabolic curvatures along circumferential direction are investigated and results are compared together. In addition, effect of variable thickness on the mode shapes is studied.

Keywords

Cylindrical shell, Parabolic curvature, Variable thickness, Natural frequency, Spline function, Discrete method.

Pouria Bahrami Ataabadi [a]
Mohammad Reza Khedmati [*] [a]
Mostafa Bahrami Ataabadi [b]

[a] Department of Marine Technology, Amirkabir University of Technology, 424 Hafez Avenue, Tehran 15916-34311, Iran
[b] Department of Engineering and Building, National Iranian Oil Company, Boushehr, 3rd Pars 75391-154, Iran

[*] Author email: khedmati@aut.ac.ir

Received 15.05.2014
In revised form 29.06.2014
Accepted 18.08.2014
Available online 26.09.2014

1 INTRODUCTION

Cylindrical (open) shells with either circular or noncircular profiles have been widely used in recent years, as structural elements within marine, civil, aerospace, and petrochemical industries. In addition, because of inherent difficulties in assembly of shells with circular profile, noncircular profile is preferred in constructing cylindrical shells. Vibration behavior of cylindrical shells with circular profile is different than that of cylindrical shells with noncircular profile.

Variation of the thickness in a cylindrical shell leads to decrease of its structural weight besides reducing cost of needed materials. Moreover, natural frequency of the shell changes as a result of its variable thickness. Therefore, vibration analysis of the shells with variable thickness has attracted the attention of many researchers in recent years.

Zhang *et al.* (2001) and Pellicano (2007) studied vibration behavior of the shells incorporating circular profile and uniform thickness. A few other researchers have also studied vibration response of noncircular shells, among them are Srinivasan and Bobby (1976), Cheung and Cheung (1972) and Yamada *et al.* (1999).

Vibration response of flat plates with variable thickness has also been addressed by Huang *et al.* (2005, 2007), Ashour (2001), Sakiyama and Huang (1998), Grigorenko *et al.* (2008). On the other hand, Sivadas and Ganesan (1991), Zhang and Xiang (2006), Duan and Koh (2008) investigated vibration response of the closed shells having circular profiles and variable thickness. Their investigations were limited to the effects of variable thickness in one direction (either axial or circumferential) on vibration behavior of the shells. Later, Grigorenko and Parkhomenko (2011) studied free vibration of shallow shells having parabolically-variable thickness with the aid of spline-collocation approach. The effects of variable thickness on the vibration behavior of closed elliptical cylindrical shells and closed oval cylindrical shells have been studied by Suzuki and Leissa (1985) and Khalifa (2011), respectively.

Open parabolic cylindrical shell with variable thickness is considered as the main geometry in the present study. As it was shown, very few research works have been performed on such structures. In addition, vibration response of parabolic cylindrical shells and circular cylindrical shells are compared against each other's. As it was mentioned earlier, most of the previous works studied the effects of thickness variation in one direction on the vibration response of the shells. Therefore, a thorough study on the effects of direction of thickness variation on the vibration response of a shell is lacked herein. Present work is aimed at study of vibration response for both parabolic shells and circular shells having variable thickness in either axial direction or circumferential direction.
On the other hand, analytical solutions cannot be simply reached for assessment of vibration response of the shells when both radius and thickness are subjected to variation. Thus, numerical approaches as well as approximate methods may be used to investigate the vibration response of these types of the shells. Techniques based on spline functions are among numerical methods that are useful in solving structural problems. In the present work, a relatively simple discrete method incorporating spline functions introduced already by Cheng and Chuang (1990) and Cheng *et al.* (1987) for shell and plate with uniform thickness and uniform curvature; is further extended to be able to analyze free vibrations of circular/noncircular cylindrical shells with variable thickness.

The aims of present work are: (1) to extend discrete method based on the concept of spline functions for studying vibration behavior of parabolic and circular cylindrical shells with non-uniform distribution of thickness and to prove its efficiency and accuracy, (2) to evaluate the effects of thickness variation along the axis of the shell on its natural frequency in comparison with those of thickness variation along the circumference of the shell on its natural frequency, (3) to compare natural frequency of cylindrical shells having circular profile with that of cylindrical shells having parabolic profile; and finally, (4) to investigate the effects of thickness variation on the mode shapes of the shells.

2 THEORY AND FORMULATIONS

Since thickness of the shell is small compared to its other dimensions, the shell is regarded to be thin. Consequently, classical shell theory based on Kirchhoff–Love assumptions is used to extract governing equations.

2.1 Geometric formulation

The main geometry under consideration in this work is a cylindrical shell with an either circular or parabolic profile. Both circular and parabolic profiles can be defined by two parameters including camber (C) and span (b), Figure 1. Geometrical relations for circular and parabolic profiles are given in Table 1.

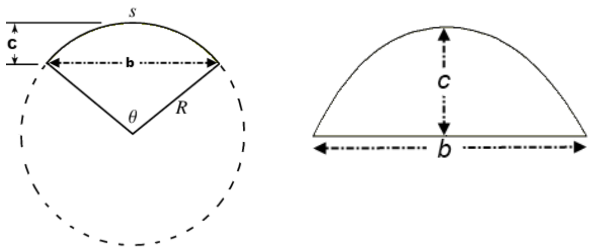

(a) (b)

Figure 1: (a) circular profile and (b) parabolic profile.

Figure 2 shows a shell with a parabolic profile in the curvilinear coordinate system (xsz). z-axis is perpendicular to the middle surface of shell defined by x-s plane. x-axis is along axis of the cylinder, while the s-axis is along circumference of the cylinder. Displacement functions along x-axis, s-axis and z-axis are respectively represented by U(x,s), V(x,s) and W(x,s). Lame's parameters for this type of shell in the curvilinear coordinate system are equal to one according to Soedel (1993).

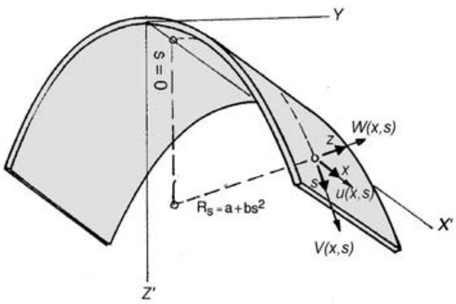

Figure 2: Parabolic cylindrical shell, curvilinear coordinate system (xsz) and displacement functions (Soedel (1993)).

2.2. Displacement functions

Displacement functions for the middle surface of the shell are introduced by cubic and fifth-order B-spline functions as below.

$$\begin{aligned} U(x,s) &= \lfloor \phi(x) \rfloor \otimes \lfloor \phi(s) \rfloor \{A\} \sin(\omega t + e) \\ V(x,s) &= \lfloor \phi(x) \rfloor \otimes \lfloor \phi(s) \rfloor \{B\} \sin(\omega t + e) \\ W(x,s) &= \lfloor \varphi(x) \rfloor \otimes \lfloor \varphi(s) \rfloor \{C\} \sin(\omega t + e) \end{aligned} \tag{1}$$

Row matrices $\lfloor \phi(x) \rfloor$ and $\lfloor \varphi(x) \rfloor$ are cubic B-spline and fifth-order B-spline matrices, respectively. Column matrices $\{A\}$, $\{B\}$ and $\{C\}$ are unknown coefficients of the displacement functions in Equation 1. Also, N is the number of divisions along x or s axes. The operator $\otimes$ is the 'Kronecker product' of the matrices. Formulations of row matrices and also column matrices are given below

$$\begin{aligned} \lfloor \phi(x) \rfloor &= \left[\phi(x)_{-1}\, \phi(x)_0\, \phi(x)_1 \ldots\ldots \phi(x)_{N-1}\, \phi(x)_N\, \phi(x)_{N+1} \right]_{N+3} \\ \lfloor \varphi(x) \rfloor &= \left[\psi(x)_{-2}\, \psi(x)_{-1}\, \psi(x)_0 \ldots\ldots \psi(x)_N\, \psi(x)_{N+1}\, \psi(x)_{N+2} \right]_{N+5} \\ \{A\}^T &= \left[\{a_{-1}\}^T \{a_0\}^T \ldots\ldots \{a_N\}^T \{a_{N+1}\}^T \right]_{[(N+3)]} \\ \{a_i\}^T &= \left[a_{i1}\ a_{i2}\ a_{i3} \ldots\ldots a_{iN} \right], i = -1,0,1,\ldots N+1 \quad ,\{B\}\ is\ same\ as \{A\} \\ \{C\}^T &= \left[\{c_{-2}\}^T \{c_{-1}\}^T \ldots\ldots \{c_{N+1}\}^T \{c_{N+2}\}^T \right]_{[(N+5)]} \\ \{c_i\}^T &= \left[c_{i1}\ c_{i2}\ c_{i3} \ldots\ldots c_{iN} \right], i = -2,-1,0,\ldots N+2 \end{aligned} \tag{2}$$

Standard cubic spline is expressed as

$$\varphi_3(x) = \frac{1}{6} \begin{cases} (2+x)^3 & x \in [-2,-1] \\ (2+x)^3 - 4(1+x)^3 & x \in [-1,0] \\ (2-x)^3 - 4(1-x)^3 & x \in [0,1] \\ (2-x)^3 & x \in [1,2] \\ 0 & |x| > 2 \end{cases} \tag{3}$$

According to Cheng *et al.* (1987), cubic B-spline functions (B_3) for N equal divisions (N>4) are

$$\begin{gathered} \phi_i = \varphi_3\left(\frac{x}{h} - i\right), i = 3,4,5\ldots,N-3 \\ \begin{aligned} \phi_{-1} &= \varphi_3\left(\frac{x}{h}+1\right) & \phi_{N-2} &= \varphi_3\left(\frac{x}{h}-N+2\right) \\ \phi_0 &= \varphi_3\left(\frac{x}{h}\right) - 4\varphi_3\left(\frac{x}{h}+1\right) & \phi_{N-1} &= \varphi_3\left(\frac{x}{h}-N+1\right) - \frac{1}{2}\varphi_3\left(\frac{x}{h}-N\right) + \varphi_3\left(\frac{x}{h}-N-1\right) \\ \phi_1 &= \varphi_3\left(\frac{x}{h}-1\right) - \frac{1}{2}\varphi_3\left(\frac{x}{h}\right) + \varphi_3\left(\frac{x}{h}+1\right) & \phi_N &= \varphi_3\left(\frac{x}{h}-N\right) - 4\varphi_3\left(\frac{x}{h}-N-1\right) \\ \phi_2 &= \varphi_3\left(\frac{x}{h}-2\right) & \phi_{N+1} &= \varphi_3\left(\frac{x}{h}-N-1\right) \end{aligned} \end{gathered} \tag{4}$$

Expression for the standard fifth-order spline is

$$\varphi_5 = \frac{1}{120}\begin{cases} (3+x)^5 & x \in [-3,-2] \\ (3+x)^5 - 6(2+x)^5 & x \in [-2,-1] \\ (3+x)^5 - 6(2+x)^5 + 15(1+x)^5 & x \in [-1,0] \\ (3-x)^5 - 6(2-x)^5 + 15(1-x)^5 & x \in [0,1] \\ (3-x)^5 - 6(2-x)^5 & x \in [1,2] \\ (3-x)^5 & x \in [2,3] \\ 0 & |x| > 3 \end{cases} \tag{5}$$

Again, according to Cheng *et al.* (1987), fifth-order B-spline functions (B_5) for N equal divisions (N>6) are

$$\begin{aligned}
\psi_i &= \varphi_5\left(\frac{x}{h} - i\right), i = 4,5,6\ldots N-4 \\
\psi_{-2} &= \varphi_5\left(\frac{x}{h} + 2\right) \\
\psi_{-1} &= \varphi_5\left(\frac{x}{h} + 1\right) - 26\varphi_5\left(\frac{x}{h} + 2\right) \\
\psi_0 &= \alpha_{11}\varphi_5\left(\frac{x}{h} + 2\right) + \alpha_{12}\varphi_5\left(\frac{x}{h} + 1\right) + \varphi_5\left(\frac{x}{h}\right) \\
\psi_1 &= \alpha_{21}\varphi_5\left(\frac{x}{h} + 1\right) + \alpha_{22}\varphi_5\left(\frac{x}{h}\right) + \varphi_5\left(\frac{x}{h} - 1\right) \\
\psi_2 &= \alpha_{31}\varphi_5\left(\frac{x}{h} + 2\right) + \alpha_{32}\varphi_5\left(\frac{x}{h}\right) + \varphi_5\left(\frac{x}{h} - 2\right) \\
\psi_3 &= \varphi_5\left(\frac{x}{h} - 3\right) \\
\psi_{N-3} &= \varphi_5\left(\frac{x}{h} - N + 3\right) \\
\psi_{N-2} &= \beta_{31}\varphi_5\left(\frac{x}{h} - N + 2\right) + \beta_{32}\varphi_5\left(\frac{x}{h} - N\right) + \varphi_5\left(\frac{x}{h} - N - 2\right) \\
\psi_{N-1} &= \beta_{21}\varphi_5\left(\frac{x}{h} - N - 1\right) + \beta_{22}\varphi_5\left(\frac{x}{h} - N\right) + \varphi_5\left(\frac{x}{h} - N + 1\right) \\
\psi_N &= \beta_{11}\varphi_5\left(\frac{x}{h} - N - 2\right) + \beta_{12}\varphi_5\left(\frac{x}{h} - N - 1\right) + \varphi_5\left(\frac{x}{h} - N\right) \\
\psi_{N+1} &= \varphi_5\left(\frac{x}{h} - N - 1\right) + 26\varphi_5\left(\frac{x}{h} - N - 2\right) \\
\psi_{N+2} &= \varphi_5\left(\frac{x}{h} - N - 2\right)
\end{aligned} \tag{6}$$

where, for cc boundary condition (clamped edges at x=0, x=L)

$$\begin{bmatrix} \alpha_{11} & \alpha_{12} \\ \alpha_{21} & \alpha_{22} \\ \alpha_{31} & \alpha_{32} \end{bmatrix} = \begin{bmatrix} \beta_{11} & \beta_{12} \\ \beta_{21} & \beta_{22} \\ \beta_{31} & \beta_{32} \end{bmatrix} = \begin{bmatrix} 165/4 & -33/8 \\ 1 & -26/33 \\ 1 & -1/33 \end{bmatrix}$$

And for ss boundary condition (simply supported edges at x=0, x=L)

$$\begin{bmatrix} \alpha_{11} & \alpha_{12} \\ \alpha_{21} & \alpha_{22} \\ \alpha_{31} & \alpha_{32} \end{bmatrix} = \begin{bmatrix} \beta_{11} & \beta_{12} \\ \beta_{21} & \beta_{22} \\ \beta_{31} & \beta_{32} \end{bmatrix} = \begin{bmatrix} 12 & -3 \\ -1 & 0 \\ -1 & 0 \end{bmatrix}$$

2.3 Mass and stiffness matrices

Extracted relations in this section are valid only for a shell with a general geometry.

2.3.1 Mass matrix

Kinetic energy of a shell with variable thickness can be expressed in the following form

$$T_{shell} = \frac{1}{2}\iint \rho_{shell} t_{shell} \left(U^2 + V^2 + W^2\right) dxds = \frac{1}{2}\{\delta\}^T [M] \{\delta\} \tag{7}$$

where, ρ_{shell} is density, t_{shell} is thickness function of shell, U, V and W are displacement functions of the middle surface of shell. Also, $\{\delta\} = [\{A\}\ \{B\}\ \{C\}]^T$, where $\{A\}$, $\{B\}$ and $\{C\}$ are unknown coefficients of displacement functions. $[M]$ is also mass matrix.

After substituting the displacement functions (Equation 1) into the Equation 7 and taking numerical integration, the mass matrix is obtained by equation 8. This mass matrix is for a shell with variable thickness in x-direction. Through replacing x by s, the mass matrix for a shell with variable thickness in s-direction can be easily obtained.

$$[M] = \rho_{shell} \begin{bmatrix} (F_{tx} \otimes F_s) & 0 & 0 \\ 0 & (F_{tx} \otimes F_s) & 0 \\ 0 & 0 & (H_{tx} \otimes H_s) \end{bmatrix} \tag{8}$$

2.3.2 Stiffness matrix

Strain energy for a shell with a general geometry can be written as follows

$$U_{shell} = \frac{1}{2}\iint \{\varepsilon\}^T [D] \{\varepsilon\} dxds = \frac{1}{2}\{\delta\}^T [K] \{\delta\} \tag{9}$$

where, the strain vector is

$$\{\varepsilon\} = \begin{bmatrix} \varepsilon_1 & \varepsilon_2 & \gamma_{12} & \chi_1 & \chi_2 & \chi_{12} \end{bmatrix}$$

The components of strain vector are

$$\begin{cases} \varepsilon_1 = \frac{1}{A_1}\frac{U}{\partial x} + \frac{1}{A_1A_2}\frac{\partial A_1}{\partial s}V + \frac{W}{R_1} \\ \varepsilon_2 = \frac{1}{A_2}\frac{V}{\partial s} + \frac{1}{A_1A_2}\frac{\partial A_2}{\partial x}U + \frac{W}{R_2} \\ \gamma_{12} = \frac{A_2}{A_1}\frac{\partial}{\partial s}\left(\frac{U}{A_2}\right) + \frac{A_1}{A_2}\frac{\partial}{\partial s}\left(\frac{V}{A_1}\right) \\ \chi_1 = -\left[\frac{1}{A_1}\frac{\partial}{\partial x}\left(\frac{U}{R_1} + \frac{1}{A_1}\frac{\partial W}{\partial x}\right) + \frac{1}{A_1A_2}\frac{\partial A_1}{\partial s}\left(\frac{V}{R_2} + \frac{1}{A_2}\frac{\partial W}{\partial s}\right)\right] \\ \chi_2 = -\left[\frac{1}{A_2}\frac{\partial}{\partial s}\left(\frac{V}{R_2} + \frac{1}{A_2}\frac{\partial W}{\partial s}\right) + \frac{1}{A_1A_2}\frac{\partial A_2}{\partial x}\left(\frac{U}{R_1} + \frac{1}{A_1}\frac{\partial W}{\partial x}\right)\right] \\ \chi_{12} = -\left[\frac{1}{A_1A_2}\left(-\frac{1}{A_1}\frac{\partial A_1}{\partial s}\frac{\partial W}{\partial x} - \frac{1}{A_2}\frac{\partial A_2}{\partial x}\frac{\partial W}{\partial s} + \frac{\partial^2 W}{\partial x \partial s}\right) + \frac{1}{R_1}\frac{A_1}{A_2}\frac{\partial}{\partial s}\left(\frac{U}{A_1}\right) + \frac{1}{R_2}\frac{A_2}{A_1}\frac{\partial}{\partial x}\left(\frac{V}{A_2}\right)\right] \\ \text{W, U, V are displacement functions} \\ R_1 \text{is radius of curvature along } X-\text{axis} \\ R_2 \text{is radius of curvature along } S-\text{axis} \\ A_1, A_2 \text{are Lame}' \text{ parameters} \end{cases}$$

Flexural rigidity of the shell is given as

$$[D] = \begin{bmatrix} B_{11}(x,s) & B_{12}(x,s) & 0 & 0 & 0 & 0 \\ B_{21}(x,s) & B_{22}(x,s) & 0 & 0 & 0 & 0 \\ 0 & 0 & B_{66}(x,s) & 0 & 0 & 0 \\ 0 & 0 & 0 & D_{11}(x,s) & D_{12}(x,s) & 0 \\ 0 & 0 & 0 & D_{21}(x,s) & D_{22}(x,s) & 0 \\ 0 & 0 & 0 & 0 & 0 & D_{66}(x,s) \end{bmatrix}$$

$$\begin{cases} B_{ii}(x,s) = \frac{E_i t(x,s)}{1-\vartheta_i\vartheta_j} \quad , \quad D_{ij}(x,s) = \vartheta_j D_{ii}(x,s) \\ B_{ij}(x,s) = \vartheta_j B_{ii}(x,s) \quad , \quad B_{66} = G_{ij} t(x,s) \\ D_{ii}(x,s) = \frac{B_{ii} t^2(x,s)}{12} \quad , \quad D_{66} = \frac{B_{66} t^2(x,s)}{6} \end{cases} \qquad \begin{matrix} E_i \textit{ is elastic modulus} \\ G_{ij} \textit{ is shear modulus} \\ t(x,s) \textit{ is thickness function} \\ \vartheta_j \textit{ is poisson's ratio} \end{matrix}$$

Stiffness matrix $[K]$ is

$$[K] = \begin{bmatrix} k_{11} & k_{12} & k_{13} \\ k_{21} & k_{22} & k_{23} \\ k_{31} & k_{32} & k_{33} \end{bmatrix}, \qquad k_{21} = k_{12}^T, k_{31} = k_{13}^T, k_{32} = k_{23}^T$$

After substituting displacement functions from the Equation 1 into the Equation 9 and taking an integration of it, components of stiffness matrix are obtained as follows

$$
\begin{aligned}
k_{11} &= \left[\left(\frac{E_1}{1-\vartheta_1\vartheta_2}\right)D_{tx}\otimes F_s + G_{12}\left(F_{tx}\otimes D_s\right)\right]\\
k_{12} &= \left[\vartheta_2\left(\frac{E_1}{1-\vartheta_1\vartheta_2}\right)E_{tx}^{T}\otimes E_s + G_{12}\left(E_{tx}\otimes E_s^{T}\right)\right]\\
k_{13} &= \left[\left(\vartheta_2+1\right)\left(\frac{E_1}{1-\vartheta_1\vartheta_2}\right)L_{tRx}^{T}\otimes G_s^{T}\right]\\
k_{22} &= \left[\left(\frac{E_2}{1-\vartheta_1\vartheta_2}\right)F_{tx}\otimes D_s + G_{12}\left(D_{tx}\otimes F_s\right)\right]\\
k_{23} &= \left[\left(\vartheta_1+1\right)\left(\frac{E_2}{1-\vartheta_1\vartheta_2}\right)G_{tx}^{T}\otimes G_{Rs}^{T}\right]\\
k_{33} &= \left[\begin{aligned}&\left(\frac{E_1}{1-\vartheta_1\vartheta_2}\right)\left(1+\vartheta_1\right)H_{tx}\otimes H_{RRs} + \left(\frac{E_2}{1-\vartheta_1\vartheta_2}\right)\left(1+\vartheta_2\right)H_{tRx}\otimes H_s\\
&+\vartheta_1\left(\frac{E_2}{12\left(1-\vartheta_1\vartheta_2\right)}\right)J_{tttx}\otimes J_s^{T} + \left(\frac{E_1}{12\left(1-\vartheta_1\vartheta_2\right)}\right)K_{tttx}\otimes H_s\\
&+\vartheta_2\left(\frac{E_1}{12\left(1-\vartheta_1\vartheta_2\right)}\right)J_{tttx}^{T}\otimes J_s + \frac{G_{12}}{6}I_{tttx}\otimes I_s + \left(\frac{E_2}{12\left(1-\vartheta_1\vartheta_2\right)}\right)H_{tttx}\otimes K_s\end{aligned}\right]
\end{aligned}
\tag{10}
$$

Some matrices are available in the list of the elements in the formulations of mass and stiffness matrices, which are called as spline matrices. Some of these spline matrices have been already derived by Cheng *et al.* (1987), while other spline matrices representing the effect of variable radius and thickness are extracted herein. Formulations of all spline matrices are presented in Table 2 and Table 3.

$F_x = \int_0^L \left[\phi(x)\right]^T \left[\phi(x)\right] dx$	$L_x = \int_0^L \left[\varphi(x)\right]^T \left[\phi'(x)\right] dx$	$I_x = \int_0^L \left[\varphi'(x)\right]^T \left[\varphi'(x)\right] dx$
$G_x = \int_0^L \left[\varphi(x)\right]^T \left[\phi(x)\right] dx$	$D_x = \int_0^L \left[\phi'(x)\right]^T \left[\phi'(x)\right] dx$	$J_x = \int_0^L \left[\varphi(x)\right]^T \left[\varphi''(x)\right] dx$
$K_x = \int_0^L \left[\varphi''(x)\right]^T \left[\varphi''(x)\right] dx$	$H_x = \int_0^L \left[\varphi(x)\right]^T \left[\varphi(x)\right] dx$	$E_x = \int_0^L \left[\phi(x)\right]^T \left[\phi'(x)\right] dx$
$Z_x = \int_0^L \left[\varphi'(x)\right]^T \left[\phi(x)\right] dx$		$S_x = \int_0^L \left[\varphi''(x)\right]^T \left[\varphi'(x)\right] dx$
Note: Through replacing x by s in these relations, spline matrices in s direction can be obtained.		

Table 2: Spline matrices used in this study and also the study of Cheng *et al.* (1987).

2.4 Frequency equation

Total potential energy for free vibration of a shell is expressed as follows

$$\Pi = \frac{2\pi}{\omega}\left[\left\{\delta\right\}^T\left(\left[K\right]-\omega^2\left[M\right]\right)\left\{\delta\right\}\right] \tag{11}$$

Substituting mass and stiffness matrices into the above equation and using the Hamilton's principle, following form of the frequency equation is obtained.

$$\left(\left[\mathrm{K}\right]-\omega^2\left[\mathrm{M}\right]\right)\left\{\delta\right\}=0 \tag{12}$$

Equation 12 is of eigenvalue type in which the eigenvalues represent the natural frequencies. Unknown coefficients of displacement functions create the eigenvectors. Solving the Equation 12 will result in the frequencies and corresponding mode shapes.

$F_{tx}=\int_0^L t(x)\lfloor\phi(x)\rfloor^T\lfloor\phi(x)\rfloor dx$	$L_{Rs}=\int_0^b\lfloor\varphi(s)\rfloor^T\lfloor\phi'(s)\rfloor ds$	$L_{tx}=\int_0^L t(x)\lfloor\varphi(x)\rfloor^T\lfloor\phi'(x)\rfloor dx$
$I_{tttx}=\int_0^L t^3(x)\lfloor\varphi'(x)\rfloor^T\lfloor\varphi'(x)\rfloor dx$	$G_{Rs}=\int_0^b\frac{\lfloor\varphi(s)\rfloor^T\lfloor\phi(s)\rfloor}{R_s}ds$	$G_{tx}=\int_0^L t(x)\lfloor\varphi(x)\rfloor^T\lfloor\phi(x)\rfloor dx$
$D_{tx}=\int_0^L t(x)\lfloor\phi'(x)\rfloor^T\lfloor\phi'(x)\rfloor dx$	$J_{Rs}=\int_0^b\frac{\lfloor\varphi(s)\rfloor^T\lfloor\varphi''(s)\rfloor}{R_s}ds$	$J_{tttx}=\int_0^L t^3(x)\lfloor\varphi(x)\rfloor^T\lfloor\varphi''(x)\rfloor dx$
$H_{RRs}=\int_0^b\frac{\lfloor\varphi(s)\rfloor^T\lfloor\varphi(s)\rfloor}{R_s^2}ds$	$H_{Rs}=\int_0^b\frac{\lfloor\varphi(s)\rfloor^T\lfloor\varphi(s)\rfloor}{R_s}ds$	$H_{tx}=\int_0^L t(x)\lfloor\varphi(x)\rfloor^T\lfloor\varphi(x)\rfloor dx$
$K_{tttx}=\int_0^L t^3(x)\lfloor\varphi''(x)\rfloor^T\lfloor\varphi''(x)\rfloor dx$	$E_{tx}=\int_0^L t(x)\lfloor\phi(x)\rfloor^T\lfloor\phi'(x)\rfloor dx$	

Note: Through replacing x by s in matrices, spline matrices in s direction can be obtained.

Table 3: Spline matrices extracted in this study.

3 NUMERICAL EXAMPLES AND DISCUSSIONS

Based on derived formulations in the previous section, a code was written in the MATLAB environment in order to calculate the natural frequencies and also corresponding mode shapes.

3.1 Verification of present method

Accuracy of presented formulations is investigated in this section in order to demonstrate its ability to analyze free vibration of both parabolic and circular cylindrical shells with either uniform or variable thickness. A comparison between natural frequencies for a circular cylindrical shell having a uniform thickness as obtained by the present method and also by Srinivasan and Bobby (1976) is given in Table 4. It should be mentioned that Srinivasan and Bobby (1976) used Rayleigh–Ritz and matrix methods in their work. On the other hand, natural frequencies as obtained by the present method and the method developed by Cheung and Cheung (1972) are provided in Table 5 for a parabolic cylindrical shell with a constant thickness. Cheung and Cheung (1972) used strip method to extract relations for vibration analysis of a cylindrical shell with parabolic profile. In Table 6 results of the present method have been compared with those of Huang *et al.* (2005) who used discrete method in combination with Green's function to obtain natural frequency solution for flat plates with variable thickness in one direction. Table 7 shows frequency parameters for a shallow shell with rectangular platform that its thickness varies parabolically in one direction (Grigorenko and Parkhomenko (2011)). Grigorenko and Parkhomenko (2011) obtained their solution method by using spline-collocation method.

Mode number	Present work			Petyt as reported in Srinivasan and Bobby (1976)		Difference (%)
	Mesh Divisions			Analysis Method		
	12×12	14×14	16×16	Extended Rayleigh-Ritz	Finite element	$100\left(\frac{\omega^{16\times16}-\omega^{\mathrm{Ref}.[3]}}{\omega^{\mathrm{Ref}.[3]}}\right)$
1st	882	879	876	870	870	-0.68
2nd	959	957	955	958	958	0.31
3rd	1297	1284	1282	1288	1288	0.46
4th	1369	1367	1366	1364	1363	-0.14
5th	1446	1444	1443	1440	1440	-0.20

$E = 1.0e7\, lb/in^2, R_s = 30\mathrm{in}, \vartheta = 0.33, a = 3\mathrm{in}, b = 4\mathrm{in}, \text{thickness} = 0.013, \rho = 0.0002484\, lbs^2/in^2, \text{B.c} = \text{CCCC}$

Table 4: Natural frequencies (Hz) for a circular cylindrical shell model (Srinivasan and Bobby (1976)).

Mode number	Present Study			Cheung and Cheung (1972)	Difference (%)
	Mesh Divisions				
	12×12	14×14	16×16		$100\left(\frac{\omega^{16\times16}-\omega^{\mathrm{Ref}.[4]}}{\omega^{\mathrm{Ref}.[4]}}\right)$
1st	0.30914	0.307773	0.30552	0.303	0.831683
2nd	0.30722	0.307101	0.30668	0.306	0.222222
3rd	0.56179	0.558907	0.55264	0.537	2.912477
4th	0.54222	0.539315	0.53974	0.538	0.32342
5th	0.56934	0.568532	0.56844	0.571	-0.44834

$E = 1, \vartheta = 0.3, a = 1\mathrm{in}, b = 1\mathrm{in}, \text{thickness} = 0.191\mathrm{in}, \rho = 1, \text{B.c} = \text{SSSS}$

Table 5: Natural frequencies (Rad/sec) for a parabolic cylindrical shell model (Cheung and Cheung (1972)).

	$b/a = 1.0$			$b/a = 0.5$		
Frequency	α			α		
parameter	0.00	0.40	0.80	0.00	0.40	0.80
$\lambda_1^{\text{Present work}}$	6.765	7.386	7.897	10.256	11.147	11.954
$\lambda_1^{\text{Huang et al. (2005)}}$	6.780	7.402	7.945	10.194	11.113	11.894
Difference (%)	-0.22	-0.21	-0.60	0.60	0.30	0.50
$\lambda_2^{\text{Present work}}$	8.944	9.708	10.468	12.171	13.286	14.386
$\lambda_2^{\text{Huang et al.(2005)}}$	8.953	9.770	10.475	12.289	13.422	14.419
Difference (%)	-0.10	-0.63	-0.06	-0.96	-1.01	-0.22
$\lambda_3^{\text{Present work}}$	10.305	11.217	12.050	15.270	16.587	17.862
$\lambda_3^{\text{Huang et al. (2005)}}$	10.293	11.232	12.046	15.301	16.695	17.908
Difference (%)	0.11	-0.13	0.03	-0.20	-0.64	-0.25
$\lambda_4^{\text{Present work}}$	11.511	12.532	13.475	16.246	17.563	18.434
$\lambda_4^{\text{Huang et al. (2005)}}$	11.615	12.679	13.610	16.131	17.476	18.511
Difference (%)	-0.89	-1.15	-0.99	0.71	0.49	-0.41

$$E_1 = 60.7e9pa, E_2 = 24.8e9pa, R_s = \infty, \vartheta_{12} = 0.23, h_0 = 0.01a, B.C = CCCC$$

$$\text{flat plate thickness} = h_0\left(1 + \alpha x/a\right), \lambda_i = \rho h_0 \omega_i^2 a^4 / \left[D_0\left(1 - \vartheta_{21}\vartheta_{12}\right)\right]$$

$$D_0 = E_2 h_0^3 / \left[12\left(1 - \vartheta_{21}\vartheta_{12}\right)\right], \ \mathit{Difference} = 100\left(\lambda^{present\ work} - \lambda^{\mathrm{Ref}}\right) / \lambda^{\mathrm{Ref}}$$

Table 6: Dimensionless frequency parameter for a flat plate with variable thickness in one direction (Huang *et al.* (2005)).

Frequency parameter λ	$\alpha = -0.4$, BC1					$\alpha = 0.4$, BC2				
	12× 12	14× 14	16× 16	18× 18	20× 20	12× 12	14× 14	16× 16	18× 18	20× 20
$\lambda_1^{\text{Present work}}$	15.58	15.57	15.57	15.56	15.56	29.58	29.55	29.53	29.53	29.52
$\lambda_1^{\text{Grigorenko (2011)}}$	16.65	16.12	15.75	15.73	15.71	30.55	30.26	30.12	29.85	29.78
Difference (%)	-6.42	-3.41	-1.14	-1.08	-0.95	-3.17	-2.34	-1.95	-1.07	-0.87
$\lambda_2^{\text{Present work}}$	37.95	37.81	37.74	37.70	37.68	48.32	48.05	47.92	47.85	47.81
$\lambda_2^{\text{Grigorenko (2011)}}$	38.36	37.99	37.44	37.34	37.33	49.32	48.64	48.43	48.09	47.91
Difference (%)	-1.06	-0.47	0.80	0.96	0.93	-2.02	-1.21	-1.05	-0.49	-0.20
$\lambda_3^{\text{Present work}}$	38.90	38.90	38.89	38.89	38.89	56.13	56.12	56.12	56.11	56.11
$\lambda_3^{\text{Grigorenko (2011)}}$	40.06	39.58	39.25	39.13	38.97	58.66	57.52	57.36	57.02	56.96
Difference	-2.89	-1.71	-0.91	-0.61	-0.20	-4.31	-2.43	-2.16	-1.59	-1.49
$\lambda_4^{\text{Present work}}$	54.18	54.09	54.04	54.01	54.00	70.75	70.59	70.52	70.48	70.46
$\lambda_4^{\text{Grigorenko (2011)}}$	54.40	54.35	54.28	54.23	54.19	71.76	71.44	71.16	70.87	70.81
Difference	-0.40	-0.47	-0.44	-0.40	-0.35	-1.4	-1.1	-0.89	-0.55	-0.49

$$E_1 = 3.68e10pa, E_2 = 2.68e10pa, G_{12} = 0.5e10pa, R_s = 12.5, R_x = 12.5, \vartheta_{12} = 0.077, h_0 = 0.04$$

$$, \mathrm{BC1: CCCC, BC2: SSSS}, h(x) = h_0\left(\alpha\left(6x^2 - 6x + 1\right) + 1\right)$$

$$\lambda_i = \omega_i a^2 \sqrt{\rho h_0 / D_{11}}, D_{11} = E_1 h_0^3 / \left[12\left(1 - \vartheta_{21}\vartheta_{12}\right)\right], \ \mathit{Difference} = 100\left[\lambda^{present\ work} - \lambda^{\mathrm{Ref}}\right] / \lambda^{\mathrm{Ref}}$$

Table 7: Dimensionless frequency parameter for a shallow shell with variable thickness in one direction (Grigorenko and Parkhomenko (2011)).

It is observed that present solution method is in sufficient agreement with the studies performed by above-mentioned researchers. Comparison results have shown the accuracy of present solution method for analyzing vibration of shells. In parallel, a convergence study was performed during the comparison analyses, based on which the number of divisions in both directions was defined to be equal to 16 for all examples.

Model ID	Profile	Geometrical properties of model	Mechanical properties of material	B.c	Thickness function
M1x	Circular	$\text{camber}(c) = 0.05\text{m}$ $\text{span of shell}(b) = 1\text{m}$ $\text{lenght of shell}(a) = 1\text{m}$	$E_x = 3.68\text{e}10\text{Pa}$ $E_s = 2.68\text{e}10\text{Pa}$ $G_{xs} = 0.50\text{e}10\text{Pa}$ $\vartheta_{xs} = 0.077$	B.c1 B.c2 B.c3	Thickness function 1
M1s					Thickness function 2
M2x	Circular	$\text{camber}(c) = 0.1\text{m}$ $\text{span of shell}(b) = 1\text{m}$ $\text{lenght of shell}(a) = 1\text{m}$	$E_x = 3.68\text{e}10\text{Pa}$ $E_s = 2.68\text{e}10\text{Pa}$ $G_{xs} = 0.50\text{e}10\text{Pa}$ $\vartheta_{xs} = 0.077$	B.c1 B.c2 B.c3	Thickness function 1
M2s					Thickness function 2
M3x	Circular	$\text{camber}(c) = 0.15\text{m}$ $\text{span of shell}(b) = 1\text{m}$ $\text{lenght of shell}(a) = 1\text{m}$	$E_x = 3.68\text{e}10\text{Pa}$ $E_s = 2.68\text{e}10\text{Pa}$ $G_{xs} = 0.50\text{e}10\text{Pa}$ $\vartheta_{xs} = 0.077$	B.c1 B.c2 B.c3	Thickness function 1
M3s					Thickness function 2
M4x	parabolic	$\text{camber}(c) = 0.05\text{m}$ $\text{span of shell}(b) = 1\text{m}$ $\text{lenght of shell}(a) = 1\text{m}$	$E_x = 3.68\text{e}10\text{Pa}$ $E_s = 2.68\text{e}10\text{Pa}$ $G_{xs} = 0.50\text{e}10\text{Pa}$ $\vartheta_{xs} = 0.077$	B.c1 B.c2 B.c3	Thickness function 1
M4s					Thickness function 2
M5x	parabolic	$\text{camber}(c) = 0.1\text{m}$ $\text{span of shell}(b) = 1\text{m}$ $\text{lenght of shell}(a) = 1\text{m}$	$E_x = 3.68\text{e}10\text{Pa}$ $E_s = 2.68\text{e}10\text{Pa}$ $G_{xs} = 0.50\text{e}10\text{Pa}$ $\vartheta_{xs} = 0.077$	B.c1 B.c2 B.c3	Thickness function 1
M5s					Thickness function 2
M6x	parabolic	$\text{camber}(c) = 0.15\text{m}$ $\text{span of shell}(b) = 1\text{m}$ $\text{lenght of shell}(a) = 1\text{m}$	$E_x = 3.68\text{e}10\text{Pa}$ $E_s = 2.68\text{e}10\text{Pa}$ $G_{xs} = 0.50\text{e}10\text{Pa}$ $\vartheta_{xs} = 0.077$	B.c1 B.c2 B.c3	Thickness function 1
M6s					Thickness function 2

MNx: model with variable thickness in x direction.

MNs: model with variable thickness in s direction.

B.c1=CCCC, B.c2=SSSS and B.c3=CSCS (x=0, a are clamped, s=0,b are simply supported).

α, in thickness function, is called thickness parameter that varies between -0.4 and 0.4

Thickness function 1 is $h(x) = h_0\left[1+\alpha\left(1+6\,x^2/a^2 - 6\,x/a\right)\right]$

Thickness function 2 is $h(s) = h_0\left[1+\alpha\left(1+6\,s^2/b^2 - 6\,s/b\right)\right]$

Table 8: General characteristics for the studied models.

3.2 Vibration analysis

In this section, vibration of circular and parabolic cylindrical panels having variable thicknesses along their circumferences or axes is studied. Three sets of the models with circular profile and also three more sets of the models with parabolic profile are constructed. Besides, each set has two subsets of the models with variable thicknesses. One subset is corresponding to the models having variable thicknesses along their circumferences (represented by MNs), while the other subset is including the models with variable thicknesses along their axes (represented by MNx). For each of the subsets, three cases for the boundary conditions are considered. General characteristics for all investigated models are introduced in Table 8. Variation of frequency parameter against thickness parameter (α) is presented in Tables 9-11 for the case of circular models. Frequency parameter for the models having a variable thickness along their axis varies in a manner completely reverse to that of the models having variable thickness along their circumference for the BC1 boundary conditions.

Model ID: M1		α								
Boundary conditions	λ	-0.4	-0.3	-0.2	-0.1	0	0.1	0.2	0.3	0.4
BC1	λ_1^{M1s}	12.200	12.448	12.671	12.871	13.104	13.203	13.337	13.448	13.538
	λ_1^{M1x}	13.953	13.754	13.546	13.334	13.120	12.907	12.698	12.493	12.296
	λ_2^{M1s}	13.610	13.880	14.233	14.472	14.650	14.722	14.935	15.031	15.123
	λ_2^{M1x}	14.763	14.741	14.717	14.689	14.655	14.616	14.568	14.511	14.440
	λ_3^{M1s}	18.039	18.138	18.196	18.202	18.064	17.917	17.775	17.634	17.496
	λ_3^{M1x}	17.330	17.500	17.653	17.790	17.992	18.019	18.111	18.188	18.213
	λ_4^{M1s}	18.598	18.474	18.341	18.233	18.244	18.231	18.193	18.132	18.046
	λ_4^{M1x}	17.774	17.923	18.040	18.128	18.209	18.229	18.244	18.239	18.250
BC2	λ_1^{M1s}	5.797	5.895	5.990	6.084	6.177	6.273	6.371	6.473	6.581
	λ_1^{M1x}	5.743	5.856	5.969	6.075	6.177	6.278	6.380	6.483	6.588
	λ_2^{M1s}	8.224	8.293	8.324	8.324	8.309	8.244	8.171	8.079	7.969
	λ_2^{M1x}	8.929	8.783	8.635	8.490	8.318	8.212	8.084	7.964	7.856
	λ_3^{M1s}	12.169	12.214	12.256	12.297	12.311	12.391	12.446	12.428	12.365
	λ_3^{M1x}	11.984	12.117	12.211	12.261	12.308	12.318	12.307	12.276	12.227
	λ_4^{M1s}	12.431	12.499	12.537	12.550	12.543	12.518	12.479	12.510	12.583
	λ_4^{M1x}	12.431	12.496	12.533	12.550	12.550	12.537	12.512	12.478	12.436
BC3	λ_1^{M1s}	7.304	7.339	7.375	7.415	7.461	7.513	7.574	7.644	7.725
	λ_1^{M1x}	6.504	6.731	6.941	7.179	7.461	7.624	7.850	8.079	8.308
	λ_2^{M1s}	9.158	9.220	9.245	9.242	9.232	9.161	9.089	9.003	8.896
	λ_2^{M1x}	9.554	9.476	9.398	9.322	9.250	9.182	9.120	9.065	9.017
	λ_3^{M1s}	14.939	14.989	15.007	14.979	14.844	14.810	14.731	14.657	14.592
	λ_3^{M1x}	13.569	13.864	14.136	14.385	14.794	14.826	15.020	15.199	15.322
	λ_4^{M1s}	15.193	15.134	15.060	14.999	14.970	14.922	14.860	14.782	14.694
	λ_4^{M1x}	14.208	14.432	14.626	14.795	14.971	15.065	15.170	15.255	15.361

$$\lambda_i = \omega_i a^2 \left(\rho h_0 / D_{11}\right)^{0.5}, D_{11} = E_1 h_0^3 / [12(1 - \vartheta_{21}\vartheta_{12})]$$

Table 9: Variation of natural frequency parameter for M1x and M1s models.

In addition, it is observed that variation of first frequency parameter against the thickness parameter is linear upwards or downwards for both of the models having variable thickness along their axis or circumference for the BC1 boundary conditions.

Model ID: M2		α								
Boundary conditions	λ	-0.4	-0.3	-0.2	-0.1	0	0.1	0.2	0.3	0.4
BC1	λ_1^{M2s}	14.379	14.478	14.56	14.619	14.643	14.776	14.822	14.854	14.872
	λ_1^{M2x}	14.766	14.723	14.692	14.661	14.644	14.583	14.571	14.569	14.528
	λ_2^{M2s}	18.007	18.402	18.752	19.062	19.112	19.570	19.772	19.942	20.077
	λ_2^{M2x}	19.882	19.662	19.548	19.481	19.113	18.68	18.245	17.878	17.543
	λ_3^{M2s}	22.478	22.421	22.341	22.243	21.917	21.990	21.837	21.666	21.475
	λ_3^{M2x}	21.223	21.407	21.553	21.697	21.909	21.976	22.040	22.082	22.144
	λ_4^{M2s}	24.017	24.114	24.180	24.220	24.235	24.227	24.197	24.146	24.072
	λ_4^{M2x}	23.937	24.070	24.163	24.216	24.234	24.220	24.168	24.098	23.9
BC2	λ_1^{M2s}	8.971	9.046	9.087	9.098	9.0759	9.0512	8.998	8.927	8.842
	λ_1^{M2x}	9.395	9.308	9.223	9.147	9.062	8.992	8.947	8.891	8.862
	λ_2^{M2s}	10.121	10.357	10.585	10.807	11.027	11.248	11.469	11.693	11.922
	λ_2^{M2x}	10.024	10.292	10.547	10.794	11.025	11.254	11.470	11.693	11.915
	λ_3^{M2s}	15.229	15.347	15.431	15.486	15.497	15.529	15.522	15.501	15.465
	λ_3^{M2x}	15.133	15.263	15.35	15.428	15.493	15.521	15.530	15.382	15.031
	λ_4^{M2s}	15.989	16.127	16.200	16.221	16.195	16.130	16.027	15.891	15.724
	λ_4^{M2x}	17.618	17.294	16.943	16.573	16.189	15.795	15.399	15.112	15.087
BC3	λ_1^{M2s}	10.275	10.355	10.400	10.416	10.388	10.379	10.331	10.266	10.186
	λ_1^{M2x}	10.272	10.286	10.305	10.339	10.392	10.427	10.487	10.553	10.645
	λ_2^{M2s}	11.485	11.682	11.880	12.081	12.247	12.499	12.719	12.951	13.193
	λ_2^{M2x}	10.835	11.195	11.552	11.899	12.242	12.581	12.937	13.272	13.626
	λ_3^{M2s}	16.656	16.794	16.869	16.892	16.869	16.806	16.707	16.574	16.410
	λ_3^{M2x}	16.705	16.959	17.183	17.397	16.872	16.734	16.375	16.011	15.658
	λ_4^{M2s}	17.548	17.650	17.714	17.748	17.757	17.745	17.712	17.663	17.598
	λ_4^{M2x}	18.719	18.386	18.029	17.653	17.748	17.947	18.126	18.293	18.443

$$\lambda_i = \omega_i a^2 \sqrt{\rho h_0 / D_{11}}, D_{11} = \frac{E_1 h_0^3}{12(1 - \vartheta_{21}\vartheta_{12})}$$

Table 10: Variation of natural frequency parameter for M2x and M2s models

Tables 9 to 11 show the variation of frequency parameter against thickness parameter for circular cylindrical shells, when their boundary conditions are of BC2 or BC3 types. In comparison with the results explained for the case of the BC1 boundary condition, the frequency parameter varies at the same manner against thickness parameter for the models having variable thickness along their axis and the models having variable thickness along their circumference, when the boundary conditions are of either BC2 or BC3 types.

From the results summarized in Tables 9 to 11, it is observed that with increase in the value of C/b for the models, frequency parameter is also increased.

Model ID: M3		α								
Boundary Conditions	λ	-0.4	-0.3	-0.2	-0.1	0	0.1	0.2	0.3	0.4
BC1	λ_1^{M3s}	16.878	16.840	16.799	16.752	16.701	16.644	16.578	16.504	16.421
	λ_1^{M3x}	16.195	16.324	16.448	16.572	16.696	16.823	16.952	17.084	17.217
	λ_2^{M3s}	18.305	18.658	18.972	19.246	19.543	19.684	19.850	19.981	20.077
	λ_2^{M3x}	21.196	20.890	20.583	20.219	19.565	19.507	19.146	18.789	18.440
	λ_3^{M3s}	25.817	25.876	25.909	25.916	25.908	25.855	25.787	25.520	25.219
	λ_3^{M3x}	25.337	25.608	25.816	25.909	25.939	25.998	25.999	25.976	25.930
	λ_4^{M3s}	26.981	26.855	26.694	26.506	26.242	26.056	25.799	25.692	25.57
	λ_4^{M3x}	25.506	25.683	25.843	26.044	26.248	26.364	26.483	26.577	26.644
BC2	λ_1^{M3s}	10.042	10.120	10.167	10.188	10.187	10.166	10.129	10.078	10.013
	λ_1^{M3x}	10.283	10.258	10.233	10.210	10.190	10.177	10.173	10.177	10.193
	λ_2^{M3s}	13.985	14.277	14.547	14.790	14.996	15.145	15.217	15.204	15.118
	λ_2^{M3x}	13.883	14.271	14.619	14.917	15.129	15.181	15.047	14.806	14.525
	λ_3^{M3s}	15.761	15.927	16.042	16.124	16.195	16.282	16.411	16.593	16.822
	λ_3^{M3x}	17.555	17.248	16.942	16.663	16.182	16.391	16.512	16.741	17.017
	λ_4^{M3s}	18.787	18.952	19.076	19.166	19.230	19.265	19.280	19.276	19.251
	λ_4^{M3x}	18.696	18.893	19.043	19.154	19.233	19.283	19.308	19.311	19.292
BC3	λ_1^{M3s}	11.767	11.862	11.923	11.956	11.966	11.954	11.924	11.877	11.815
	λ_1^{M3x}	11.471	11.535	11.674	11.818	11.970	12.132	12.304	12.490	12.690
	λ_2^{M3s}	15.450	15.679	15.882	16.047	16.162	16.217	16.211	16.152	16.047
	λ_2^{M3x}	14.762	15.266	15.727	16.121	16.260	16.343	16.154	15.905	15.578
	λ_3^{M3s}	16.603	16.810	16.982	17.143	17.475	17.515	17.749	18.015	18.308
	λ_3^{M3x}	18.291	18.030	17.777	17.569	17.503	17.688	18.047	18.475	18.934
	λ_4^{M3s}	20.960	21.111	21.216	21.285	21.321	21.331	21.315	21.276	21.214
	λ_4^{M3x}	20.012	20.383	20.721	21.034	21.324	21.595	21.849	22.089	22.316

$$\lambda_i = \omega_i a^2 \sqrt{\rho h_0 / D_{11}}, D_{11} = \frac{E_1 h_0^3}{12\left(1-\vartheta_{21}\vartheta_{12}\right)}$$

Table 11: Variation of natural frequency parameter for M3x and M3s models.

In Tables 12 to 14, variation of frequency parameter against thickness parameter (α), for parabolic models is presented. Similar to the results for circular models, it is observed herein also that with any increase in the value of C/b for the models with parabolic profile, frequency parameter increases. The tendencies of the variation of frequency parameter for the models having parabolic profile are the same as those for the models having circular profile. Nevertheless, frequency parameter for the parabolic models is greater than that for the circular models, as confirmed also in Cheung and Cheung (1972).

Model ID: M4		α								
Boundary Conditions	λ	-0.4	-0.3	-0.2	-0.1	0	0.1	0.2	0.3	0.4
BC1	λ_1^{M4s}	12.295	12.545	12.771	12.973	13.151	13.308	13.471	13.556	13.648
	λ_1^{M4x}	14.111	13.908	13.696	13.480	13.181	13.044	12.649	12.620	12.416
	λ_2^{M4s}	13.787	13.960	14.114	14.356	14.836	14.884	14.946	15.011	15.250
	λ_2^{M4x}	14.974	14.955	14.933	14.908	14.878	14.843	14.723	14.746	14.680
	λ_3^{M4s}	18.108	18.206	18.274	18.315	18.227	18.089	17.923	17.816	17.683
	λ_3^{M4x}	17.596	17.767	17.921	18.059	18.211	18.289	18.363	18.382	18.353
	λ_4^{M4s}	18.744	18.626	18.498	18.364	18.339	18.318	18.256	18.224	18.141
	λ_4^{M4x}	17.931	18.080	18.195	18.288	18.342	18.377	18.403	18.462	18.525
BC2	λ_1^{M4s}	5.927	6.026	6.120	6.215	6.309	6.405	6.486	6.606	6.7155
	λ_1^{M4x}	5.8735	5.990	6.099	6.205	6.308	6.409	6.451	6.615	6.720
	λ_2^{M4s}	8.336	8.405	8.437	8.436	8.418	8.356	8.245	8.191	8.081
	λ_2^{M4x}	9.043	8.896	8.748	8.602	8.441	8.324	8.142	8.076	7.966
	λ_3^{M4s}	12.297	12.343	12.387	12.432	12.477	12.529	12.526	12.511	12.459
	λ_3^{M4x}	12.121	12.255	12.349	12.411	12.445	12.456	12.420	12.414	12.365
	λ_4^{M4s}	12.523	12.592	12.630	12.643	12.636	12.611	12.646	12.653	12.729
	λ_4^{M4x}	12.526	12.590	12.627	12.644	12.644	12.630	12.591	12.570	12.528
BC3	λ_1^{M4s}	7.432	7.467	7.504	7.545	7.592	7.645	7.685	7.777	7.859
	λ_1^{M4x}	6.633	6.861	7.086	7.309	7.592	7.756	7.871	8.209	8.440
	λ_2^{M4s}	9.266	9.328	9.355	9.350	9.321	9.270	9.184	9.109	9.005
	λ_2^{M4x}	9.666	9.587	9.508	9.432	9.359	9.290	9.229	9.170	9.122
	λ_3^{M4s}	15.033	15.084	15.102	15.095	15.025	14.944	14.885	14.798	14.736
	λ_3^{M4x}	13.705	14.000	14.271	14.520	14.999	15.061	15.269	15.335	15.413
	λ_4^{M4s}	15.310	15.254	15.183	15.105	15.065	15.021	14.913	14.879	14.790
	λ_4^{M4x}	14.305	14.528	14.722	14.890	15.036	15.160	15.312	15.347	15.498

$$\lambda_i = \omega_i a^2 \sqrt{\rho h_0 / D_{11}}, D_{11} = \frac{E_1 h_0^3}{12\left(1-\vartheta_{21}\vartheta_{12}\right)}$$

Table 12: Variation of natural frequency parameter for M4x and M4s models.

Model ID:M5 Boundary Conditions	λ	α -0.4	-0.3	-0.2	-0.1	0	0.1	0.2	0.3	0.4
BC1	λ_1^{M5s}	14.838	14.956	15.063	15.169	15.254	15.322	15.414	15.438	15.465
	λ_1^{M5x}	15.471	15.413	15.348	15.286	15.234	15.187	15.153	15.123	15.115
	λ_2^{M5s}	19.295	19.795	19.966	20.042	20.066	20.641	21.047	21.272	21.463
	λ_2^{M5x}	20.839	21.014	20.798	20.443	20.062	19.668	19.325	18.822	18.383
	λ_3^{M5s}	22.732	22.728	22.652	22.586	22.494	22.389	22.311	22.17	21.939
	λ_3^{M5x}	20.416	20.123	20.169	20.615	20.962	21.515	21.593	21.673	21.736
	λ_4^{M5s}	25.254	25.381	25.477	25.535	25.571	25.583	25.549	25.534	25.456
	λ_4^{M5x}	25.320	25.451	25.535	25.575	25.577	25.541	25.470	25.366	25.227
BC2	λ_1^{M5s}	9.595	9.6724	9.714	9.726	9.714	9.680	9.575	9.556	9.4718
	λ_1^{M5x}	10.071	9.985	9.882	9.794	9.7235	9.639	9.5134	9.513	9.466
	λ_2^{M5s}	10.942	11.183	11.415	11.641	11.864	12.086	12.237	12.533	12.758
	λ_2^{M5x}	10.846	11.118	11.362	11.617	11.841	12.073	12.419	12.527	12.745
	λ_3^{M5s}	15.635	15.756	15.842	15.900	15.934	15.950	15.943	15.931	15.900
	λ_3^{M5x}	15.616	15.739	15.822	15.884	15.920	15.948	15.945	15.937	15.772
	λ_4^{M5s}	16.668	16.805	16.880	16.902	16.880	16.818	16.633	16.593	16.436
	λ_4^{M5x}	18.323	17.999	17.648	17.275	16.887	16.487	16.081	15.672	15.471
BC3	λ_1^{M5s}	10.864	10.944	10.992	11.007	10.999	10.970	10.902	10.858	10.778
	λ_1^{M5x}	10.941	10.946	10.954	10.965	10.991	11.022	11.075	11.123	11.197
	λ_2^{M5s}	12.297	12.502	12.706	12.912	13.123	13.340	13.593	13.798	14.041
	λ_2^{M5x}	11.687	12.052	12.406	12.761	13.119	13.450	13.831	14.155	14.574
	λ_3^{M5s}	17.336	17.471	17.543	17.565	17.543	17.481	17.397	17.255	17.339
	λ_3^{M5x}	17.288	17.523	17.754	17.971	17.543	17.269	17.059	16.754	16.376
	λ_4^{M5s}	17.966	18.070	18.137	18.175	18.188	18.181	18.136	18.111	18.053
	λ_4^{M5x}	19.295	18.992	18.629	18.246	18.197	18.280	18.454	18.614	18.758

$$\lambda_i = \omega_i a^2 \sqrt{\rho h_0 / D_{11}}, D_{11} = \frac{E_1 h_0^3}{12\left(1-\vartheta_{21}\vartheta_{12}\right)}$$

Table 13: Variation of natural frequency parameter for M5x and M5s models.

Model: M6		α								
Boundary conditions	λ	-0.4	-0.3	-0.2	-0.1	0	0.1	0.2	0.3	0.4
B.c1	λ_1^{M6s}	17.763	17.532	17.202	17.103	17.023	17.026	17.022	17.011	16.994
	λ_1^{M6x}	16.670	16.761	16.850	16.941	17.037	17.140	17.251	17.321	17.501
	λ_2^{M6s}	20.153	20.505	20.846	21.126	21.364	21.563	21.721	21.840	21.921
	λ_2^{M6x}	23.397	23.046	22.666	22.265	21.350	21.126	20.998	20.577	20.150
	λ_3^{M6s}	26.854	26.762	26.646	26.507	26.346	26.167	25.966	25.748	25.505
	λ_3^{M6x}	25.442	25.715	25.956	26.170	26.360	26.528	26.675	26.806	26.914
	λ_4^{M6s}	27.292	27.415	27.502	27.555	27.575	27.562	27.511	27.440	27.328
	λ_4^{M6x}	27.429	27.588	27.696	27.759	27.783	27.772	27.730	27.668	27.564
B.c2	λ_1^{M6s}	10.611	10.694	10.745	10.768	10.770	10.752	10.718	10.668	10.605
	λ_1^{M6x}	10.929	10.887	10.846	10.808	10.774	10.746	10.727	10.717	10.717
	λ_2^{M6s}	15.480	15.823	16.136	16.364	16.511	16.361	16.263	16.129	15.962
	λ_2^{M6x}	15.225	15.644	16.035	16.397	16.553	16.479	16.145	15.803	15.464
	λ_3^{M6s}	16.315	16.447	16.536	16.652	16.960	17.203	17.521	17.845	18.177
	λ_3^{M6x}	18.269	17.945	17.608	17.274	17.019	17.195	17.519	17.852	18.185
	λ_4^{M6s}	18.622	18.799	18.937	19.041	19.119	19.174	19.208	19.223	19.221
	λ_4^{M6x}	18.644	18.822	18.956	19.054	19.122	19.164	19.183	19.182	19.162
B.c3	λ_1^{M6s}	12.229	12.325	12.389	12.424	12.435	12.426	12.399	12.355	12.296
	λ_1^{M6x}	11.974	12.084	12.195	12.313	12.439	12.574	12.721	12.879	13.052
	λ_2^{M6s}	16.651	16.942	17.157	17.270	17.394	17.256	17.172	17.052	16.899
	λ_2^{M6x}	16.111	16.645	17.146	17.353	17.444	17.347	17.039	16.725	16.417
	λ_3^{M6s}	17.419	17.577	17.749	17.977	18.283	18.567	18.897	19.246	19.611
	λ_3^{M6x}	18.991	18.706	18.417	18.177	18.309	18.743	19.218	19.705	20.200
	λ_4^{M6s}	20.807	20.975	21.099	21.189	21.248	21.281	21.292	21.281	21.250
	λ_4^{M6x}	20.013	20.364	20.683	20.977	21.248	21.501	21.736	21.957	22.163

$$\lambda_i = \omega_i a^2 \sqrt{\rho h_0 / D_{11}}, D_{11} = \frac{E_1 h_0^3}{12\left(1-\vartheta_{21}\vartheta_{12}\right)}$$

Table 14: Variation of natural frequency parameter for M6x and M6s models.

From the obtained numerical results, the following observations can be summarized:

- With increase in C/b (b is constant and C varies), frequency of all models (circular and parabolic profiles) is increased. With increase in C/b, arc length of both profiles will increase, and then weight of models increases. In addition, the increase of camber (C) will decrease radius of curvature of shells. Increase in the weight of the models decreases the natural frequency and also decrease of the radius of curvature increases the natural frequency of models. Therefore, effect of the change in the curvature on the natural frequency is greater than the effect of change in the weight for studied models. The tendencies of variation of frequency parameter are the same for both circular and parabolic models. Nevertheless, for the models with the same values of C/b, the natural frequency in case of parabolic curvature is greater than that in case of circular curvature. This phenomenon may be due to the facts that; (1) local stiffness of parabolic models is greater than local stiffness of circular models and (2) weight of circular models is greater than parabolic models with the same C/b (because the arc length of circular profile is greater than the arc length of parabolic profile).
- Effect of thickness variation along both directions on the natural frequency is studied. It was aimed to find out the difference between effect of thickness variation along direction with zero curvature (x direction) and effect of thickness variation along direction with nonzero curvature (s direction). It is observed that for the case of BC1 boundary condition, the frequency parameter variation for the models with variable thickness along their axis is in opposite tendency compared with the models having variable thickness along their circumference.
- Effect of boundary condition on natural frequency is studied for three cases. It can be seen that the effect of boundary condition on natural frequency is greater than the effect of variable thickness on natural frequency. Models with BC1 boundary condition have largest natural frequency and models with BC2 boundary condition have lowest natural frequency. In addition, boundary condition changes the manner of frequency parameter variation against the thickness parameter. For example, for the BC1 type of boundary condition, frequency parameter varies linearly against thickness parameter but for the BC2 and BC3 types of boundary condition, frequency parameter varies nonlinearly against thickness parameter.

3.3 Effect of variable thickness on the mode shapes

Eigen vectors of the Equation 13 are unknown coefficients of the displacement functions. By finding these unknown coefficients, the relevant mode shapes can be plotted. The effect of thickness parameter on the first four mode shapes is studied herein for the models M5s and M5x (both models have parabolic profiles). Figure 3 shows the effect of thickness parameter on the first four mode shapes for the model M5x (the parabolic cylindrical shell with variable thickness along x axis). In general, for the first and third modes, the mode shapes visually are similar to each others for different values of the thickness parameter. For negative (-) and positive (+) values of the thickness parameter (α), the second and fourth modes have equal numbers of half waves but the way the half waves are appeared is opposite. Figure 4 shows the effect of thickness parameter on the mode shapes for the M5s model (the parabolic cylindrical shell with variable thickness along s axis). As can be observed, the thickness parameter does not have any significant effect on the mode shape for M5s model.

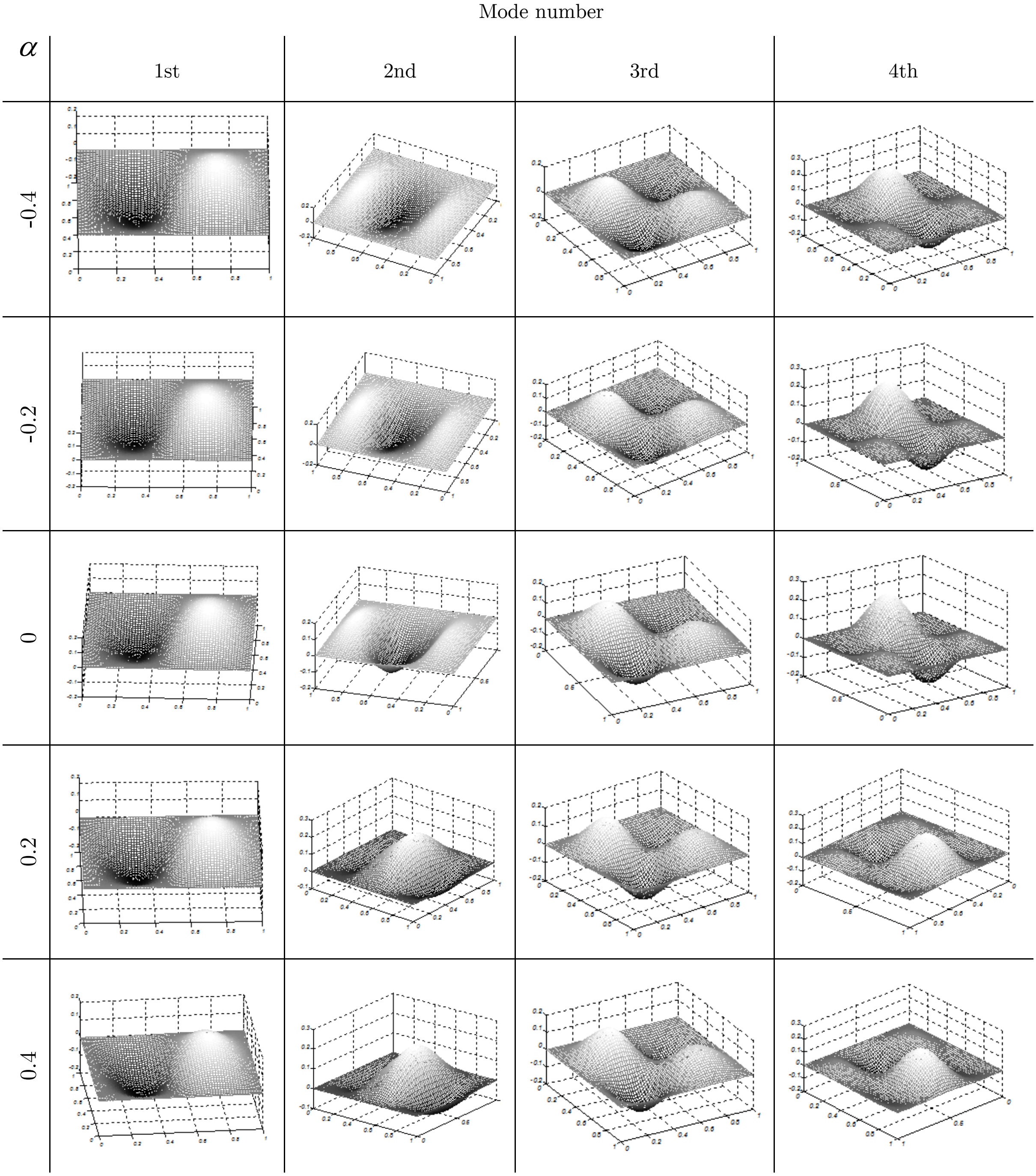

Figure 3: Effect of thickness parameter (α) on the mode shapes for the parabolic model with $c/b = 0.15$ (Model M6s).

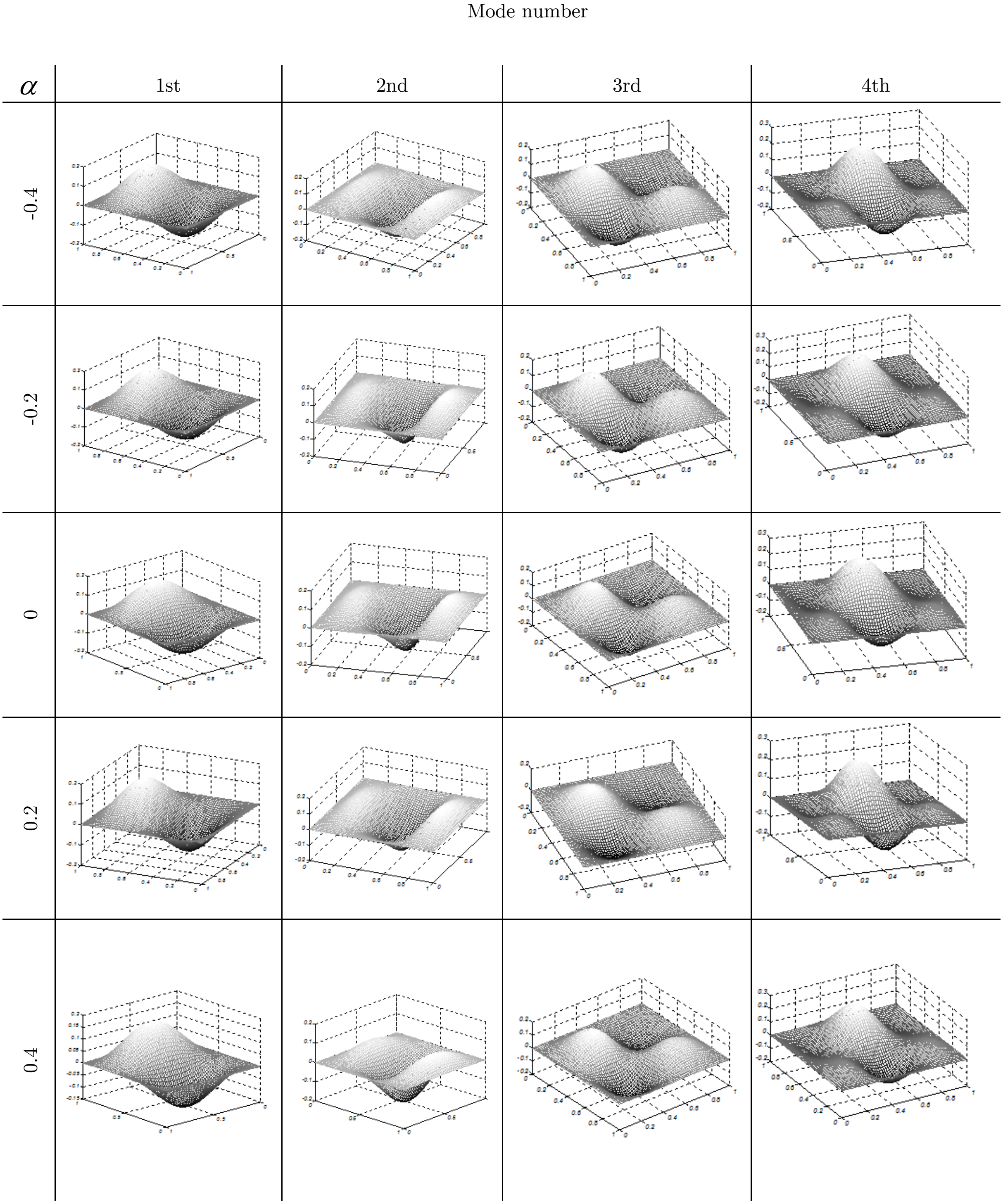

Figure 4: Effect of thickness parameter (α) on the mode shapes for the parabolic model with $c/_{b} = 0.15$ (Model M6x).

4 CONCLUSIONS

An approximate analysis method for investigating the free vibration behavior of circular and parabolic cylindrical shells having variable thickness along their axis or circumference is presented. A finite element method based on B-spline functions is further extended to find out the natural frequencies and corresponding mode shapes for the cylindrical shells with variable radii of curvature and non-uniform thicknesses. Usefulness and accuracy of the present method is demonstrated through comparison of the results for a variety of cases. It is observed that frequency parameter for circular models vary in the same way against thickness parameter as that for parabolic models. Moreover, natural frequency of cylindrical models with a parabolic profile is slightly greater than that of cylindrical models with a circular profile.

References

Ashour, A.S., (2001). A semi-analytical solution of the flexural vibration of orthotropic plates of variable thickness, Journal of Sound and Vibration 240: 431–445.

Cheng, S.P., Chuang, D., (1990). Dynamic analysis of stiffened plates and shells using spline gauss collocation method, Computers & Structures 36: 623-629.

Cheng, S.P., Dade, H., Zongmu, W., (1987). Static, vibration and stability analysis of stiffened plates using B spline functions, Computers & Structures27:73-78.

Cheung, Y. K., Cheung, M.S., (1972). Vibration analysis of cylindrical panels, Journal of Sound and Vibration 22: 59-73.

Duan, W., Koh, C., (2008). Axisymmetric transverse vibrations of circular cylindrical shells with variable thickness, Journal of Sound and Vibration 317: 1035–1041.

Grigorenko, A.Y., Parkhomenko, A.Y., (2011). Free Vibration of Shallow Orthotropic Shells with Variable Thickness and Rectangular platform, Journal of International Applied Mechanics 46: 877-889.

Grigorenko, Y.M., Grigorenko, A.Y., Efimova, T.L., (2008). Spline-based investigation of natural vibrations of orthotropic rectangular plates of variable thickness within classical and refined theories, Journal of Mechanics of Materials and Structures 3: 929-952.

Huang, M., Ma, X.Q., Sakiyama, T., Matsuda, H., Morita, C., (2005). Free vibration analysis of orthotropic rectangular plates with variable thickness and general boundary conditions, Journal of Sound and Vibration 288: 931-955.

Huang, M., Ma, X.Q., Sakiyama, T., Matsuda, H., Morita, C., (2007). Free vibration analysis of rectangular plates with variable thickness and point supports, Journal of Sound and Vibration 300: 435-452.

Khalifa, A.M., (2011). Simplified equations and solutions for the free vibration of an orthotropic oval cylindrical shell with variable thickness, Math. Meth. Appl. Sci 34: 1789-1800.

Pellicano, F., (2007). Vibrations of circular cylindrical shells: theory and experiments, Journal of Sound and Vibration 303: 154–170.

Sakiyama, T., Huang, M., (1998). Free vibration analysis of rectangular plates with variable thickness, Journal of Sound and Vibration 216: 379–397.

Sivadas, K., Ganesan, N., (1991). Free vibration of circular cylindrical shells with axially varying thickness, Journal of Sound and Vibration 147: 73–85.

Soedel, W. (1993). Vibration of Shells and plates, Marcel Dekker INC.

Srinivasan, R.S., Bobby, W., (1976). Free vibration of noncircular cylindrical shell panels, Journal of Sound and Vibration 46: 43-49.

Suzuki, K., Leissa, A., (1985).Free vibrations of noncircular cylindrical shells having circumferentially varying thickness, Journal of Applied Mechanics52: 149–154.

Yamada, G., Irie, T., Notoya, S., (1999). Natural frequencies of elliptical cylindrical shells, Journal of Sound and Vibration 101: 133–139.

Zhang, L., Xiang, Y., (2006). Exact solutions for vibration of stepped circular cylindrical shells, Journal of Sound and Vibration 299: 948–964.

Zhang, X., Liu, G., Lam, K., (2001). Vibration analysis of thin cylindrical shells using wave propagation approach, Journal of Sound and Vibration 239: 397–403.